

# Three-dimensional MHD simulation of the solar wind from the solar surface to 400 solar radius using REPPU (REProduce Plasma Universe) code

---

## Mitsue Den<sup>1</sup>

National Institute of Information and Communications Technology  
4-2-1 Nukui-Kitamachi, Koganei, Tokyo 184-8795, Japan  
E-mail: den@nict.go.jp

## Takashi Tanaka

Kyushu University  
156-2 Green Hill Terada, 432 Terada-machi, Hachioji, Tokyo, Japan  
E-mail: tatanaka@serc.kyushu-u.ac.jp

## Yuki Kubo

National Institute of Information and Communications Technology  
4-2-1 Nukui-Kitamachi, Koganei, Tokyo 184-8795, Japan  
E-mail: kubo@nict.go.jp

## Shinichi Watari

National Institute of Information and Communications Technology  
4-2-1 Nukui-Kitamachi, Koganei, Tokyo 184-8795, Japan  
E-mail: watari@nict.go.jp

Three-dimensional MHD simulation code, REPPU (REProduce Plasma Universe) code, is developed for modeling of space plasma phenomena, and is utilized for the solar surface and the global solar wind structure. The distinguishing features of this code is the 3-D grid system, which has no polar singularity though it is able to fit the spherical structure. This grid system makes it possible to set fine grids on the inner boundary of the inner simulation region which corresponds to the solar surface. Magnetic field structure on the solar surface is significantly important for the solar disturbances because it determines the global structure of the solar wind. REPPU code achieved both the implementations for the fine grid structure on the inner boundary and for the wide range grids in global solar wind configuration. We extend the outer boundary to 400 solar radius, though the previous our model covered 200 solar radius. We split the simulation region at several 10 solar radius where the solar wind speed is super-sonic. The simulation model for the inner region is developed in a rotational frame and the observed magnetic field data are input on the solar surface as the inner boundary. The frame of the simulation model for the outer region is a fixed frame and simulation data in the inner region are set at the inner boundary of this code. This improvement made it possible to perform stable simulation in the outer region where rotational component of the solar wind velocity is high. We describe REPPU code and present several simulation results.

*The 34th International Cosmic Ray Conference  
30 July- 6 August, 2015*

---

<sup>1</sup>Speaker

The Hague, The Netherlands

## 1. Introduction

It is well known that coronal mass ejections (CMEs) and high speed stream from coronal holes (CHs) could have huge effects on space environment near Earth. Prediction of geoeffectiveness due to these phenomena is important and primary goal for space weather. CMEs are burst phenomena observed on the solar corona and CHs are the region on the solar surface where is relatively low temperature, low density and ejects high stream. Modeling of full propagation is necessary to investigate the impact on the space environment, however it is challenging on the view of numerical simulations. One of the most difficulties is large difference in dynamical scales. Time step is determined near the Sun, and calculation with this time step in the interplanetary region takes much simulation resources such as CPU times. There are several MHD models developed from outer region about 20 - 50 solar radii to several AU (Odstrcil, Hayashi) or the photosphere to the interplanetary space (Nakamizo et al. 2009, hereafter Work1, Toth, Usmanov, Lionello). We developed three-dimensional MHD simulation code, REPPU (REProduce Plasma Universe) code, and utilized for the solar surface and the global solar wind structure. This code is similar with the previous code used in Work1, however, we extend the outer boundary to 400 solar radii, while the previous model covered 200 solar radii. We split the simulation region at several 10 solar radii where the solar wind speed is super-sonic. The simulation model for the inner region is developed in a rotational frame and the observed magnetic field data are input on the solar surface as the inner boundary. The frame of the simulation model for the outer region is a fixed frame and data calculated in the inner region are set at the inner boundary of this code. This improvement made it possible to perform stable simulation in the outer region where rotational component of the solar wind velocity is large. In this paper, we describe REPPU code and present several simulation results.

## 2. Method

We present the equations of motion for describing MHD. In our method, magnetic field  $\mathbf{B}$  is divided into time independent photospheric potential field  $\mathbf{B}_0$  and time-varying field  $\mathbf{B}_1$ . The set of governing equations is as follows,

$$\frac{\partial \rho}{\partial t} + \nabla \cdot (\rho \mathbf{v}) = 0 \quad , \quad (1)$$

$$\frac{\partial (\rho \mathbf{v})}{\partial t} + \nabla \cdot \left( \rho \mathbf{v} \mathbf{v} + P \mathbf{I} + \frac{B^2 - B_0^2}{2\mu_0} \mathbf{I} - \frac{\mathbf{B} \mathbf{B} - \mathbf{B}_0 \mathbf{B}_0}{\mu_0} \right)$$

$$= -\rho \frac{GM_s}{r^2} \hat{\mathbf{r}} - 2\rho \boldsymbol{\Omega} \times \mathbf{r} - \rho \boldsymbol{\Omega} \times (\boldsymbol{\Omega} \times \mathbf{r}) + S_M \quad , \quad (2)$$

$$\frac{\partial \mathbf{B}_1}{\partial t} = \nabla \times (\mathbf{v} \times \mathbf{B}) \quad , \quad (3)$$

$$\begin{aligned} & \frac{\partial U_1}{\partial t} + \nabla \cdot \left[ \mathbf{v} \cdot \left( U_1 + P + \frac{B_1^2}{2\mu_0} \right) - \frac{\mathbf{B}_1(\mathbf{v} \cdot \mathbf{B}_1)}{2\mu_0} - \frac{\mathbf{B}_0(\mathbf{v} \cdot \mathbf{B}_1)}{2\mu_0} + \frac{\mathbf{v}(\mathbf{B}_1 \cdot \mathbf{B}_0)}{2\mu_0} \right] \\ & = \rho \mathbf{v} \cdot \left( -\frac{GM_s}{r^2} \hat{\mathbf{r}} \right) - \rho V \cdot [\boldsymbol{\Omega} \times (\boldsymbol{\Omega} \times \mathbf{r})] + S_E, \end{aligned} \quad (4)$$

and

$$U_1 = \frac{\rho v^2}{2} + \frac{P}{\gamma - 1} + \frac{B_1^2}{2\mu_0}, \quad (5)$$

where

$$\mathbf{B} = \mathbf{B}_0 + \mathbf{B}_1,$$

and  $\rho, v, p, T$  are the plasma density, velocity, pressure and temperature respectively.  $U_1$  is modified total energy density,  $\mu$  is the magnetic permeability of vacuum,  $G$  the gravitational constant,  $M_s$  the solar mass,  $\boldsymbol{\Omega}$  the angular frequency velocity, and  $\gamma$  the ratio of specific heat given as  $\gamma = 5/3$ . The  $S_M$  in Eq. (2) and the  $S_E$  in Eq. (4) represent the momentum and energy source terms, respectively. Since the detailed mechanism of heating the solar corona and accelerating the solar wind are not fully understood, we assume these terms as follows,

$$S_E = Q \exp(-R/L_Q) + \nabla \cdot \left( \xi T^{2.5} \frac{\nabla T \cdot \mathbf{B}}{B^2} \right) \cdot \mathbf{B}, \quad (6)$$

$$S_M = M \exp(-R/L_M). \quad (7)$$

The  $S_E$  consists of a volumetric heating function (the first term) and the Spitzer-type thermal conduction (the second term),  $Q$  and  $L_Q$  are the intensity and e-folding decay length the external heat source, and  $\xi$  is the coefficient of the parallel thermal conductivity. The intensity  $Q$  is assumed to be depend on the expansion factor of the magnetic field,  $f_s$ . The  $S_M$  is also given in a similar form of the heating function in Eq. (6) so  $Q$  and  $L_M$  are the intensity and e-folding decay length the external heat source. Those parameters and functions are

$$Q = Q_0 \cdot \frac{1}{f_s}, \quad f_s = \left( \frac{R_s}{R} \right)^2 \frac{B_{R_s}}{B_R}, \quad M = M_0 \cdot \frac{1}{f_s}$$

with

$$Q_0 = 3.3 \times 10^{-6} \text{ Jm}^{-3} \text{ s}^{-1}, \quad M_0 = 5.3 \times 10^{-14} \text{ Nm}^{-3}, \quad L_Q = L_M = 0.9R_s$$

where  $B_{R_s}$  is the magnetic field at the solar surface.

As mentioned in the previous section, our mesh structure is unstructured grid and has no singularities on the poles (see Work 1) which contributes to stabilization of calculations and prevents the time step from getting finer near the poles. We adopt the 4th level grids here, which has 1922 grid points on the sphere. We set 200 grid points for the inner region and 80 points for the outer region in the radial direction. To integrate eqs (1) – (4) in time, we use the finite volume TVD scheme (Tanaka, 1994, and references therein) with third order accuracy in space.

To prepare the initial condition, we use the line-of-sight photospheric magnetic field data provided by the Wilcox Solar Observatory (WSO) and calculate a Dirichlet problem to obtain the 3D potential magnetic field. Other variables are solved with Neumann conditions.  $\mathbf{B}_1$  is set to be 0 at the initial time and  $\rho = 1.5 \times 10^{-13} \text{ kgm}^{-3}$  and  $T = 0.5 \times 10^6 \text{ K}$  on the photosphere. The velocity on the photosphere is set to be parallel to be the magnetic field and the condition is  $\partial V_{//} / \partial r_{//} = 0$  where  $//$  indicates parallel to the magnetic field. The details of the initial conditions and the boundary conditions are same as those in Work 1.

In order to simulate the wide region beyond the Earth orbit, we split our simulation region at the distance where the solar wind is supersonic. Here we set this region at 100 solar radii. The inner region is simulated in a rotational frame with the solar rotation and the outer region in a rest frame. Simulated data in the inner region are set on the inner boundary of the outer region simulation to connect two simulation models. This method make possible modeling from the solar surface, determining the solar wind structure, to 400 solar radii, about two times large as distance to the Earth.

### 3. Simulation Result

Figures 1 (a) – (c) are simulation results with used of Wilcox data CR1913. Figure 1 (a) shows 3D magnetic neutral sheet neat the Sun with orange color, color contour of the temperature on the solar surface, magnetic field lines reaching the earth orbit in red color and magnetic field lines not reaching the earth orbit in white color. Figures (b) and (c) are zoomed out from Fig (a). Blue colored sections on the solar surface indicate low temperature regions, which are corresponding to the CHs. It is interesting that curved neutral sheet is concerned with the CH at the low latitude. Many red lines start from the low latitude region, however, it should be noted that there are the red lines originating from the CH located at the high latitude. This means that not only the CHs placed at the low latitude also the CHs at the high latitude could have an effect on the environment near the earth.

Figures 2 (a) and (b) present distribution of the solar wind speed in color contour on the equatorial plane ((a)) and on the meridional plane ((b)) which covered from the solar surface to 400 solar radii. We confirm that the 3D global structure of the solar wind could be reasonably simulated.

Figures 3 (a)-(e) are synoptic chart of the magnetic field on the photosphere ((a)), open magnetic field at 2.5 solar radii ((b)), temperature at 213 solar radii (about distance from the sun to L1 point) ((c)), the solar wind speed at 213 solar radii ((d)) and observation data of the solar wind velocity and temperature obtained by the ACE spacecraft ((e)). The initial magnetic field data is that for CR2161 (Feb. 28-Mar. 26) including St. Patrick event. One of features is that the period for high-speed solar wind continued for about 6 days, comparatively long term and is thought to be one of cause of the long geomagnetosphere disturbance. That high-speed stream seemed to be ejected from the CH on the southern solar surface and we can see that high-speed region in southern hemisphere starting on March 16 in Fig. 3 (d). It is noted that simulation data on the white horizontal line indicating about 7 degree solar latitude in southern hemisphere in (c) and (d) should be compared with the observation data when taking account of the inclination of a plane of revolution. Figure 3 (c) showed that the high-speed region almost agreed with high temperature region, and this indicates that the origin of the stream was the CH. The corresponding region can be seen in Fig.3 (b), which is also consistent with the high-speed stream origin. Beginning of the high-speed stream is earlier about one day and that stream lasting period is shorter than the observation data. We consider that there are two main reasons for this discrepancy. One would be the ambiguities in the acceleration model of the solar wind adopted here given in Eqs. (6) and (7). These equations include the parameters which cannot be determined uniquely, and this model is based on a kind of empirical rule. The other is that our simulation reproduces the ambient solar wind while the CME propagation and interaction with the solar wind occurred in the period. This could have a major effect on the difference of the results.

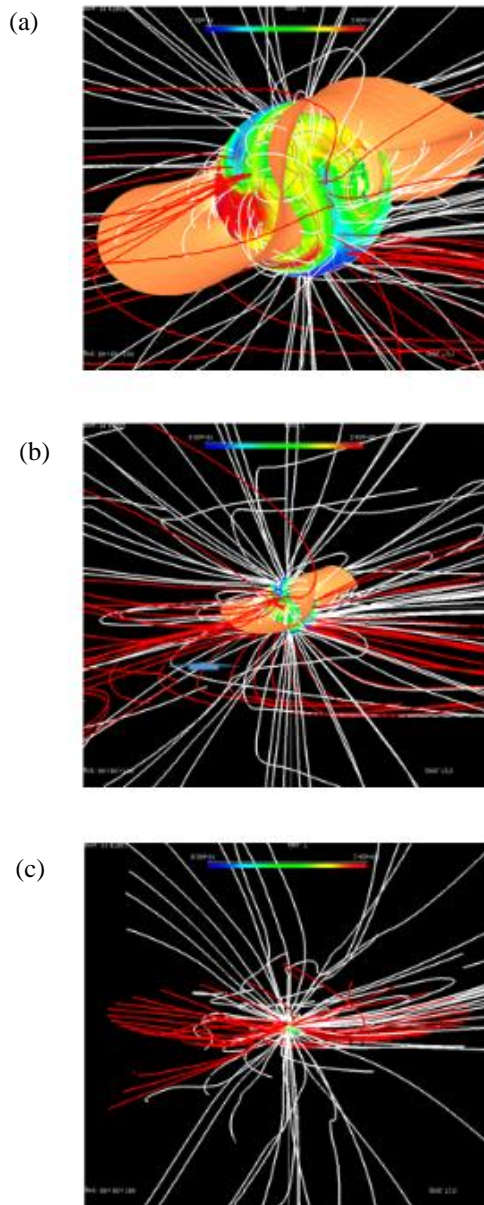


Figure 1 Simulation results on the solar surface (a) and zoomed out (b) and (c). Color shading shows temperature, orange color neutral sheet, red lines magnetic field line reaching the earth orbit and white line magnetic field line not reaching the earth orbit.

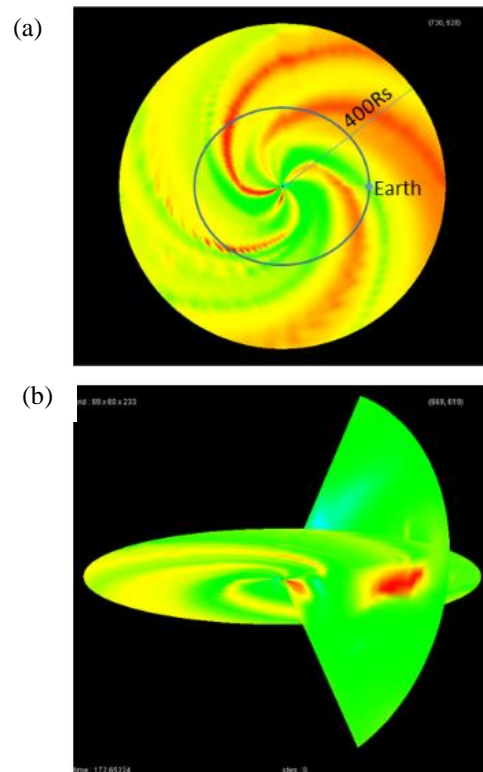


Figure 2 Color contour indicates distribution of the solar wind velocity simulated from the solar surface to 400 solar radii. (a) presents the equatorial plane and (b) the meridional plane.

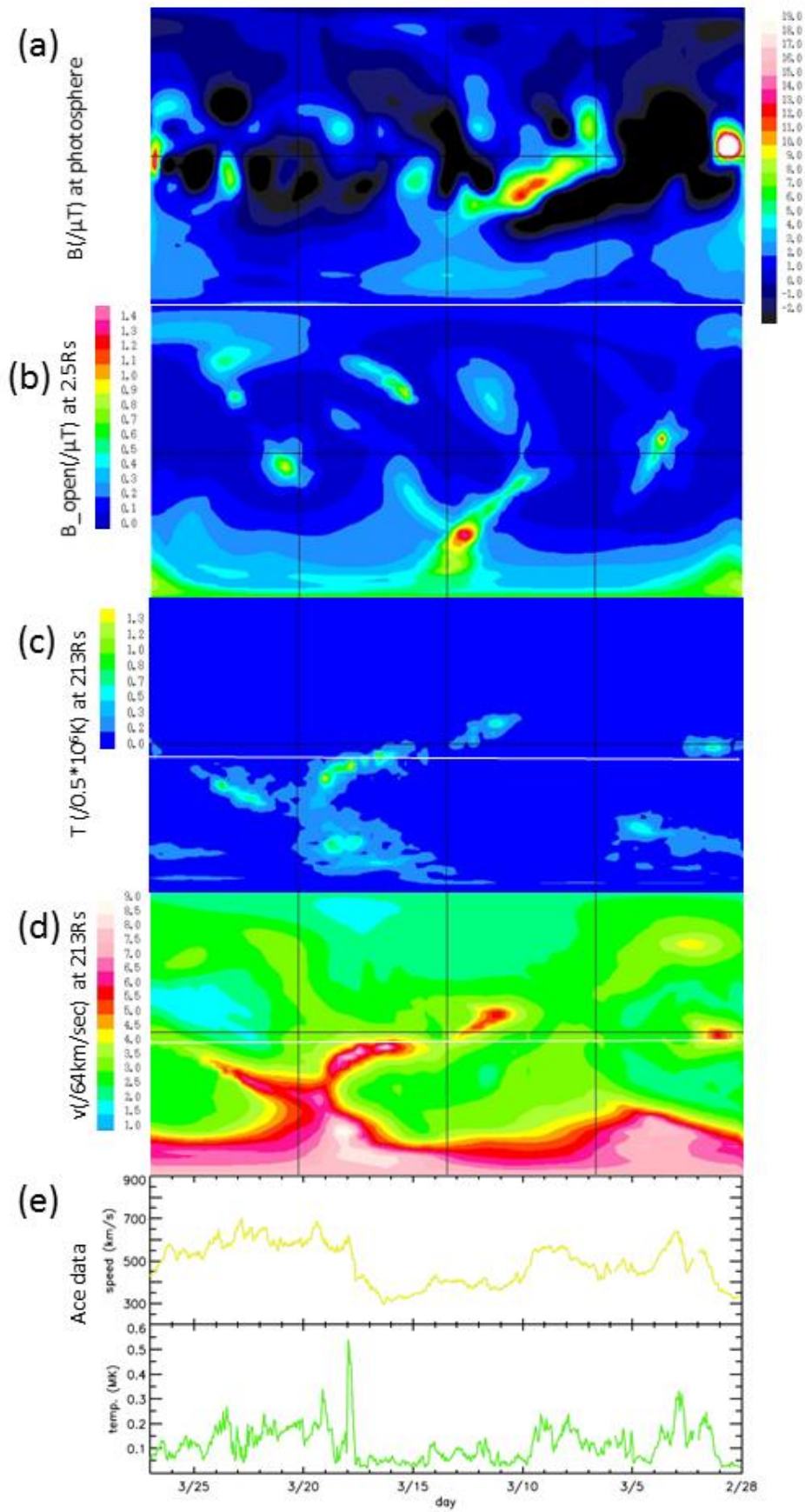


Figure 3 Synoptic chart (longitude in horizontal axis and latitude in vertical axis) of (a) simulation result of magnetic field on the photosphere, (b) that of open magnetic field at 2.5 solar radii, (c) temperature distribution at 213 solar radii, and (d) the solar wind velocity at 213 solar radii. (e) shows observation velocity and temperature data obtained by the ACE spacecraft for the corresponding period.

#### 4. Discussion and Conclusion

We developed the 3D MHD simulation model, REPPU code, for the solar surface and the global solar wind structure. The 3-D grid system of this code has no polar singularity though it is able to fit the spherical structure, which makes it possible to set fine grids on the inner boundary which corresponds to the solar surface. REPPU code achieved both the implementations for the fine grid structure on the inner boundary and for the wide range grids in global solar wind configuration. We extend the outer boundary to 400 solar radii. We split the simulation region at 100 solar radii in this paper. Simulation results including the period when St. Patrick event occurred were presented. Though the term of high-speed solar wind are slightly different from that of observation data, comparatively long term for lasting of the high-speed stream and the origin of that stream could be well reproduced in our simulations. That difference might be due to the ambiguities in the acceleration model of the solar wind and to that our simulation does not include the effect of CMEs at current state. Our code could identify that the source of the stream might be the CH in southern surface of the sun since our model could simulate from the solar surface.

We are preparing for operation to forecast the solar wind condition by using this code. It is expected to be useful for prediction of recurrent disturbance. Furthermore we will input CME models in order to model propagation of CME and predict the arrival time of shock wave associated with the CME in future which is one of primary purposes of space weather forecast.

#### References

- [1] D. Odstrcil, V. J. Pizzo and C. N. Arge, 2205, JGRA, 110, 2106.
- [2] K. Hayashi, 2012, JGRA, 117, 8105.
- [3] A. Nakamizo, T. Tanaka, Y. Kubo, S. Kmaei, H. Shimazu and H. Shinagawa, 2009, JGRA, 114, A07109.
- [4] G. Toth, I. V. Sokolov, T.I. Gombosi, et al., 2005, JGRA, 110, 12226.
- [5] A. V. Usmanov and M. L. Goldstein, 2006, JGRA, 111, 7101.
- [6] R. Lionello, C. Downs, J. A. Linker, et al., 2013, JGRA, doi:10.1088/0004-637X/777/1/76..
- [7] T. Tanaka, JCP, 1994, 111, 381..